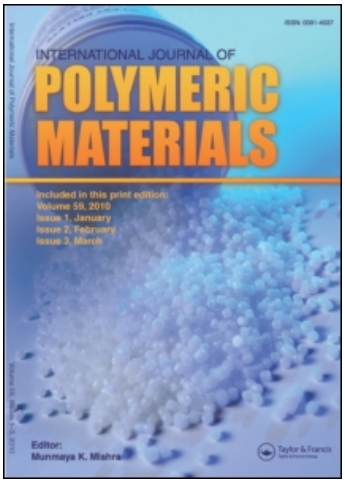

International Journal of Polymeric Materials
Publication details, including instructions for authors and subscription information:
http://www.informaworld.com/smpp/title~content=t713647664

Investigation of Weakly Oriented Polymeric Objects by Extended Fringe Field Interference Method

A. M. Sadik[a]; D. Litwin[b]
[a] Physics Department, Faculty of Science, University of Mansoura, Mansoura, Egypt [b] Institute of Applied Optics, Warsaw, Poland

To cite this Article Sadik, A. M. and Litwin, D.(2009) 'Investigation of Weakly Oriented Polymeric Objects by Extended Fringe Field Interference Method', International Journal of Polymeric Materials, 58: 10, 517 — 532
To link to this Article: DOI: 10.1080/00914030903081505
URL: http://dx.doi.org/10.1080/00914030903081505

International Journal of Polymeric Materials, 58:517–532, 2009

ISSN: 0091-4037 print/1563-535X online
DOI: 10.1080/00914030903081505

Taylor & Francis
Taylor & Francis Group

Investigation of Weakly Oriented Polymeric Objects by Extended Fringe Field Interference Method

A. M. Sadik[1] and D. Litwin[2]
[1]Physics Department, Faculty of Science, University of Mansoura, Mansoura, Egypt
[2]Institute of Applied Optics, Warsaw, Poland

An extended interferometric method is suggested to increase the measuring accuracy of the spectral dispersion curves of weakly oriented polymeric objects. This extended method is based on the variable-wavelength interferometry fringe field interference (VAWIFFI). Using this method, the calculation of the initial interference order is more accurate, and it can be determined over a small range of the visible spectrum. The advantage of the extended VAWIFFI method is that it is not necessary to take a certain reference like the zero order fringe and/or the initial coincident configuration. In comparison to the single- and multi-fringe VAWIOFT and Pluta methods, the measurement accuracy of the extended VAWIFFI method is discussed.

Keywords: extended interferometric method, polarizing, refractive index, spectral dispersion, variable-wavelength, weakly oriented

INTRODUCTION

Precise measurement of the spectral dispersion of polymeric material has a special interest to researchers who work in the field of polymer science and technology. Interferometry has been widely employed and creates potential industrial applications. Important information on tested polymeric materials related to their physical and chemical properties can be extracted using different interferometric methods.

Received 27 April 2009; in final form 5 May 2009.

The authors would like to thank Professor Dr. A. A. Hamza, Faculty of Science, University of Mansoura, Egypt for fruitful discussions.

Address correspondence to A. M. Sadik, Physics Department, Faculty of Science, University of Mansoura, 35516 Mansoura, Egypt. E-mail: adelsa_12@yahoo.com

The crucial problem of any measuring technique involving interferometry is the determination of the interference order in the image of the object under study. The variable-wavelength interferometry, which has been developed by many researchers, is one of the most successful approaches [1–12]. Pluta applied three different developed methods to determine the initial and current interference orders in the images of fringe field, uniform fringe field and optical Fourier transform of the highly birefringent under study [4,6]. These methods are based on a selection of such a particular wavelength for which interference fringes displaced by the birefringent object under study become consecutively coincident and anticoincident with the reference (undisplaced) fringes. The global errors in measurement of the initial interference order and the spectral dispersion of optical parameters were estimated and found to be ± 1 and 10^{-3}, respectively. Sometimes, it is necessary to change the initial interference order m_1 in the image of the highly oriented polymeric object by ± 3 to obtain the correct dispersion curve [6]. This undesirable effect and the precise measurement of the current wavelength requires reconfiguring of the optical system each time, which is inconvenient and slows down significantly the measurement procedure significantly.

Sadik and Litwin applied three modified interferometric methods based on variable-wavelength interferometry optical Fourier transform (VAWIOFT) for initial and current interference orders measurement in the image of highly oriented polymeric objects [8,10,11]. The advantages of these methods are that the evaluation is simple, the processing time is short, and there is not any confusion with identification of the interference orders. Therefore, the global errors in optical path difference and birefringence measurements were found to be $\pm 7 \times 10^{-3}\lambda$ and 21×10^{-5}, respectively.

All the above-mentioned methods can not apply for weakly oriented polymeric objects which produce a number of consecutive fringe coincidences, which are less than 2. Hamza et al. suggested an interferometric method based on the fringe field interference variable-wavelength interferometry for determination of the initial interference order in the image of low birefringent fiber [12]. The disadvantage of this method is that the position of the initial coincidence is needed and the value of initial interference order is approximated to be an integer number. Moreover, such a task was performed manually and the global error of directional refractive indices and birefringence is about $\pm 10^{-3}$.

The main aim of the present work is to overcome these problems using an extended interferometric method. This method is based on variable-wavelength fringe field interference (VAWIFFI) technique

for investigating weakly oriented polymeric objects. Using this method, there is no need to start with or obtain the coincident and anticoincident positions for measurement of the initial interference order as in conventional interferometric methods [6,12]. This leads to the decrease of the global error in the determination of the initial interference order in the image of the weakly oriented polymeric object. Besides, this extended VAWIFFI method can be applied for moderate and highly oriented objects (fibers, thin films, layers, and others).

In addition, in this paper, the variable-incidence angle interferometric method is used to overcome the problem of the thickness determination uncertainty [13,14]. This means that it is not necessary to calibrate the system when the image processing system is used for measuring the fringe deflections and interfringe spacing in the object image and empty field, respectively.

THEORY

The main concept of the variable-wavefront shear double-refracting microinterferometer is based on the influence of Wollaston prisms in the transmitted light [4]. This interferometer is composed of crossed polarizer "P" and analyzer "A" with two Wollaston prisms as shown in Figure 1. A light wave with a plane wavefront Σ_p, is polarized linearly by the polarizer P. On passing through the object under study, the wave is subjected to a local phase retardation corresponding to the optical path difference δ produced by the object O. Then, the wavefront Σ_p is split into two wavefronts Σ_e and Σ_o. These distorted wavefronts Σ_e and Σ_o enter the objective Ob. Also, they are laterally sheared by the first prism W_o and then additionally by W_2 into two separate wavefronts Σ_e and Σ_o, polarized at right angles to one another. The Wollaston prism W_o produces a phase shift (Δ) between both ordinary-extraordinary ($\Sigma_o - \Sigma_e$) and extraordinary-ordinary ($\Sigma_e - \Sigma_o$) waves as shown in Figure 1. On passing through the analyzer A, both wavefronts interfere with each other, produce fringe pattern in the image plane, and make visible the object O in the form of two images O'_e and O'_o. The wavefront shear S depends on the magnifying power of the objective and the size of the object under study. The fringes reach their maximum contrast when the axis of the Wollaston prism (W_o) is located at 45° with respect to the polarizer axis.

The resultant intensity (I) of light transmitted by the analyzer is given by:

$$I = 2\tau^2 I_o \sin^2\left(\frac{\pi}{\lambda}\delta(x,y)\right) \tag{1}$$

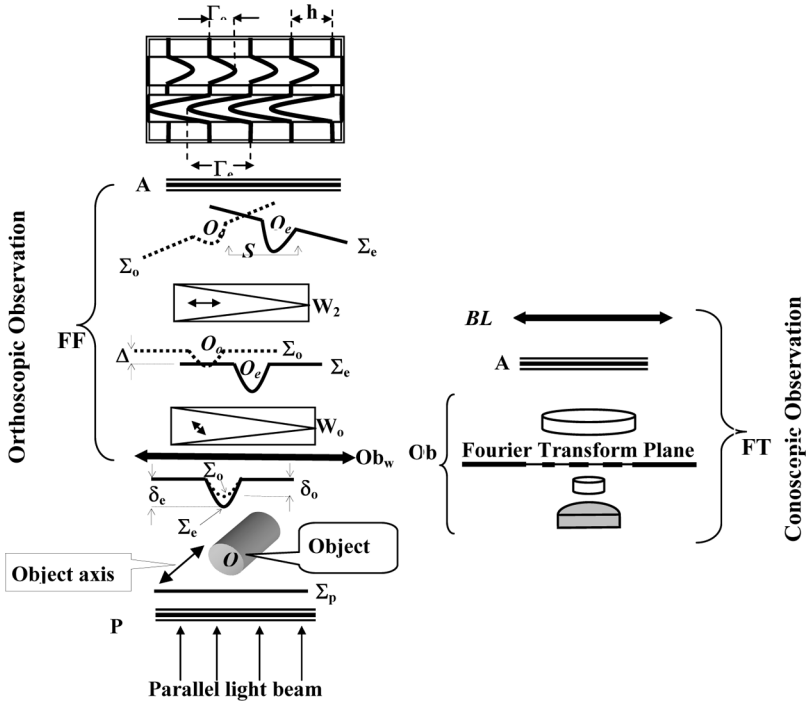

FIGURE 1 Schematic diagram of the double-refracting polarizing interference microscope used for: 1) illustrating basic notation for fringe interference produced by two plane wavefronts Σ_o and Σ_e inclined at angle to each other, 2) conoscopic and orthoscopic observations of the fringe field interference and the optical Fourier transforms of the birefringent fibers, respectively; P – polarizer, D – condenser diaphragm, C – condenser, A– analyzer; LCF – Lyot tunable birefringent filter, FT and FI – optical parts are used for conoscopic and orthoscopic observations, respectively, Ob – normal objective lens, Obw – Wallston objective lens, BL – Bertrand lens, W_o – rotatable Wollaston prism, W_2 – tube Wollaston prism.

where, τ is the intensity transmittance of the polars, I_o is the intensity of unpolarized light and $\delta(x,y)$ is the optical path difference produced by the birefringent object which is given by:

$$\delta(x,y) = \frac{\Gamma(x,y)}{h}\lambda = m\lambda = d(n_e - n_o), \tag{2}$$

where, h is the interfringe spacing and $\Gamma(x,y)$ is the fringe deflection in the object image.

Eq. (1) can be rewritten as:

$$I_N = \sin^2 \pi \frac{\delta}{\lambda} = \sin^2 \pi \frac{d \cdot B}{\lambda}, \tag{3}$$

where, I_N ($=I_\perp/2I_o\tau^2$) is normalized to unity ($0 \le I_N \le 1$).

Let us select a wavelength λ_1 as long as possible for which $I_N = 0$ and $\delta/\lambda = \delta_1/\lambda_1 = m_1$. Then, the wavelength is diminished within the visible spectrum up to the violet region and the consecutive wavelengths λ_2, λ_3, $\lambda_4 \ldots$ are recorded for which $I_N = 1, 0, 1, \ldots$ and $\delta/\lambda = \delta_s/\lambda_s = m_1 + q_s$. For all interference sequences (dark fringes), the optical path difference changes from i λ to $(i+1)\lambda$, where i is the number of consecutive fringe coincidences ($=1, 2, 3 \ldots, n$). Let the wavelength of the light be continuously varied from λ_1 (long wavelength) to λ_s (short wavelength) through the entire visible spectrum. After some simple manipulations it is possible to calculate the initial interference order (m_1) and the birefringence of the object can be written as follows:

$$m_1 = (i + q_s) \frac{\lambda_s}{\frac{(n'_e - n'_o)_s}{(n'_e - n'_o)_1}\lambda_1 - \lambda_s} \tag{4-a}$$

and;

$$B_s = \frac{(m_1 + i + q_s)\lambda_s}{d}, \tag{4-b}$$

where, n'_e and n'_e are the ordinary and extraordinary indices of refraction of the tube birefringent prism, $q_s \left(= \frac{Z_s - h_s}{h_s}\right)$ is the digital increment or decrement of the current interference order with respect to $(m_1 + i)$, and Z_s is the fringe displacement inside the image of the object related to neighbor empty fringe (liquid fringe).

The directional refractive indices n_{js} of the object under study can be calculated using the following equation:

$$n_{js} = \frac{(m_{j1} + i + q_{js})\lambda_s}{d} + n_{Ls};\ j = \begin{cases} e & \text{extraordinary beam} \\ o & \text{ordinary beam} \end{cases} \tag{5}$$

where, n_{Ls} is the refractive index of the surrounding medium, $m_{j1} \left(= (i + q_{js}) \frac{\lambda_s}{\Delta n_{js1}\lambda_1 - \lambda_s}\right)$ is the initial interference order in the ordinary and/or extraordinary images of the object, and $\Delta n_{js1} \left(= \frac{n_{js} - n_{Ls}}{n_{j1} - n_{L1}} \approx 1\right)$ is

the coefficient which expresses the degree of similarity of the spectral dispersions of the refractive indices n_j and n_L.

However, it is necessary to know the thickness of the object to calculate the refractive index and the birefringence. In this context, the variable-incident angle technique is potentially very helpful.

The main existing error in the determination of the refractive index and the birefringence is due to uncertainty in the measuring of the object thickness. Even high accuracy of optical path difference can not compensate for the lack of accuracy in the measurement of diameter of the object. For this reason, the variable-incident angle technique is combined with the variable-wavelength techniques to determine the object thickness at three different incidence angles of monochromatic light using the equation:

$$d = \frac{\sin^2\theta_1\left(\delta_{\theta_2}^2 - \delta_{\theta_0}^2\right) + \sin^2\theta_2\left(\delta_{\theta_0}^2 - \delta_{\theta_1}^2\right)}{2n_L\sin^2\theta_1(\delta_{\theta_0} - \delta_{\theta_2}\cos\theta_2) + 2n_L\sin^2\theta_2(\delta_{\theta_1}\cos\theta_1 - \delta_{\theta_0})}, \quad (7)$$

where, $\delta_{\theta_0}, \delta_{\theta_1}$ and δ_{θ_3} are the optical path differences for a given incidence angles θ_0, θ_1 and θ_2, respectively.

EXPERIMENTAL

Measuring Technique

The basic optical elements of the optical system of variable-wavefront shear double-refracting polarizing interference (PI) microscope are shown in Figure 1, whose diagram illustrates the fringe field interference and the optical Fourier transform methods. Two essential optical parts, FF and FT of the PI microscope, are used for orthoscopic (FFI) and conoscopic (OFT) observations, respectively. With the exception of these optical parts, all the optical elements are the same for FFI and OFT techniques. The Bertrand lens BL is used together with the ocular, for observation of conoscopic images in the exit pupil (Fourier transform plane) of the objective. For conoscopic observation the slit S of the condenser diaphragm D is oriented parallel to the fiber axis, but in case of observation of nonduplicated and duplicated FFI pattern (orthoscopic observation), the slit S is oriented to the fiber axis by an angle 90° and 135° or 45°, respectively. The polarizer P and analyzer A are crossed and their directions of light vibrations make an angle of 45 degrees with the principal axis of the object. The FFI and OFT patterns of the output field of the microscope are captured by a CCD camera for further automatic processing and analysis using two

different software programs. More details about the description of the automatic image analysis systems are given elsewhere [15].

RESULTS AND DISCUSSION

The double-refracting polarizing interference microscope is adapted for orthoscopic observation (FFI method) as shown in Figure 1. The fiber is immersed in a liquid of high viscosity ($n_L = 1.53538 \pm 2 \times 10^{-5}$) at temperature 27°C. When the objective birefringent Wollaston prism (W_o) is crossed with the tube birefringent prism (W_2), wavefront shear fringe field interference ($\lambda = 546$ nm) with totally duplicated (extraordinary and ordinary) images of, for example, Nylon 6 fibers with draw ratios 1.0 and 2.2 are obtained as shown in Figure 2(a and b). Also, the objective prism (W_o) can be oriented substractively in relation to W_2 and a nonduplicated interference images can be obtained as shown in Figures 2(c and e).

Concrete values of the directional refractive indices and birefringence of the object can be determined from the optical path difference that is directly measured if the object thickness is known. Unfortunately, accurate measurement of the thickness is not trivial even when modern image processing techniques are employed. The Nylon 6 fiber thickness can be determined precisely when the optical system is adapted to the variable-incidence angle interference method [13]. The Nylon 6 fibers with draw ratios D = 1.0, 2.2 are put on the upper plate of the variable prismatic device and placed in the object plane of

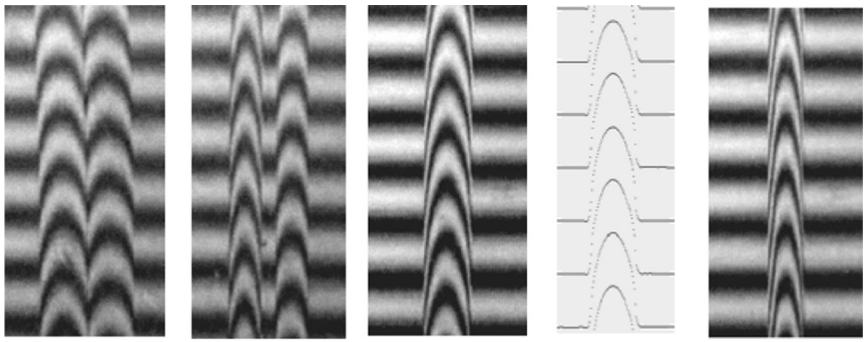

FIGURE 2 Fringe field interference patterns of Nylon 6 fibers with draw ratios 1.0 (a, c) and 2.2 (b, e); Objective prism W_o is adjusted at the crossed (a, b) and subtractive (c, e) in relation to the tube birefringent prism W_1. (d) is the skeletonizing of interferograms (c) ($\lambda = 546$ nm).

the polarized microscope and transilluminated normally by the monochromatic light. It is not necessary to translate the pixels to the real values in microns when this technique and the interference formula (Eq. (6)) are applied. Therefore, the thickness of the Nylon 6 fibers can be simultaneously determined using Eq. (6) by measuring the fringe displacements (Γ_e) at three different incidence angles. By solving the system of three equations, the thickness of Nylon 6 fiber with draw ratios 1.0 and 2.2 were found to be 31.92 μm and 22.07 μm ± 0.17, respectively.

It is important to note that the global error in thickness measurement (Δd) is decreased and found to be $\pm 17 \times 10^{-2}$. Using Eq. (2), the influence of thickness and optical path difference errors (Δd and $\Delta\delta$) on the global error of the fiber refractive index $\Delta n_j \left(= \sqrt{(\Delta n_L)^2 + \left(\frac{\delta_j \Delta d}{d^2}\right)^2 + \left(\frac{\Delta \delta_j}{d}\right)^2} \right)$ can be studied. Table 1 demonstrates that the error in measuring the fiber thickness is critical. Also, the measurement of the optical path difference with a high accuracy can not compensate for the lack of accuracy in measurement of fiber thickness. For this reason, the method based on the changing of the angular position of the fiber in respect to the axis of the optical system was used successfully to overcome this limitation.

When the wavelength varied from long to short-wavelength, the fringe displacement in the Nylon 6 fiber nonduplicated images is increased. The measurement of the initial and current interference orders can be carried out using the extended VAWIFFI method. The fringe interference patterns were processed and skeletonized by a thinning procedure and the fringe deflections in the fiber images were measured automatically. Figure 2(d) shows the skeletonizing of interferograms 2(c) by using a thinning procedure.

TABLE 1 Influence of Diameter and Optical Path Difference Errors on Accuracy of the Refractive Index of the Fiber

	Δd (μm)			
	1	0.5	0.1	0.05
$\Delta\delta_j$ (μm)	$\Delta n = \sqrt{(\Delta n_L)^2 + \left(\frac{\delta_j \Delta d}{d^2}\right)^2 + \left(\frac{\Delta \delta_j}{d}\right)^2}$			
$\lambda/50$	0.001020	0.000539	0.000224	0.000206
$\lambda/100$	0.001005	0.000510	0.000142	0.000112
$\lambda/500$	0.001000	0.000500	0.000102	0.000055

$\lambda = 0.5\,\mu m$; $n_L = 1.55$; $\delta n_L = 10^{-5}$; $d = 50\,\mu m$; $n_j = 1.6$

The fringe deflection Z_s between the displaced fringes in the fiber image and undisplaced fringes of the same order of the liquid fringes can be measured as a function of light wavelength (λ). The difficulty in the measurement of $Z_s(\lambda)$ lies in the fact that this magnitude should be determined at the midpoint of the examined interference fringes in the fiber image as precisely as possible. So, the measurement of the fringe deflection for a given wavelength is performed between as many fringes as possible for the part of the length of the fiber under study. Having measured $Z_s(\lambda)$ and $h_s(\lambda)$, the digital increment (q_s) of the interference order with respect to the initial interference order can be determined. Using the extended VAWIFF method (Eq. (4a)), the initial interference order is a digital number because it is not necessary to start with a certain particular wavelength and coincident configuration. The initial interference order in the images of the Nylon 6 fibers with draw ratios 1.0 and 2.2 was determined over a small range of spectrum and found to be 1.772 and 1.970, respectively, where $i = 1, 2$. Finally, the spectral dispersions of the birefringence and the refractive

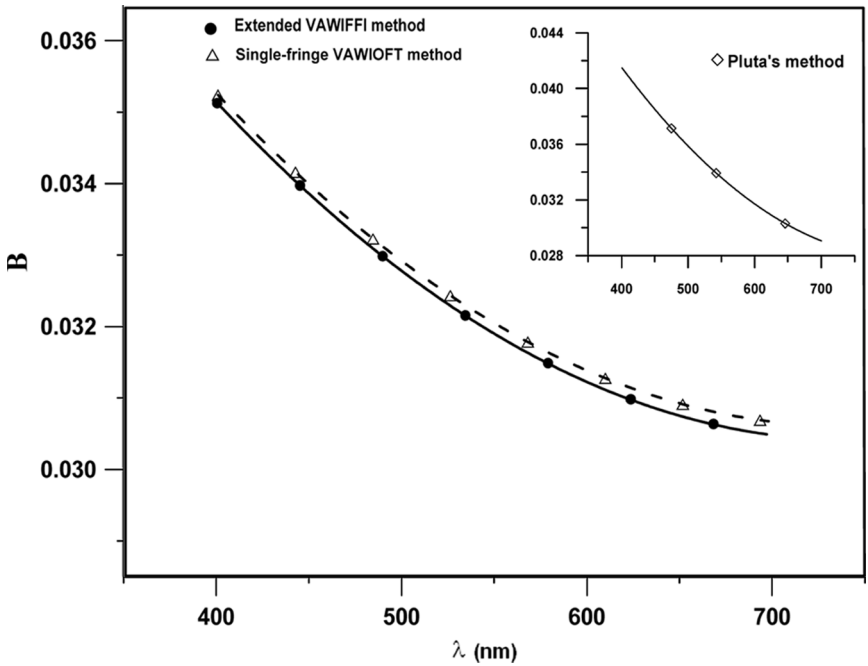

FIGURE 3 Spectral dispersion of the birefringence $B(\lambda)$ of the Nylon 6 fiber with a draw ratio 1.0 using extended VAWIFFI, single-VAWIOFT and Pluta methods.

indices of the Nylon 6 fibers with draw ratios 1.0 and 2.2 were calculated over the whole visible spectrum using the extended VAWIFFI method (Eqs. (4b) and (5)) as shown in Figures 3–5. The global error in birefringence ΔB (d, δ) and refractive index Δn (d, $n_{L,}$ δ) measurements using the extended VAWIFFI method was estimated and found to be $\pm 24 \times 10^{-5}$. The measurements of the spectral dispersions of these optical parameters has been determined using the single- and multi-fringe VAWIOFT and Pluta methods for a comparative study.

When Pluta's method [6] is applied, the number of consecutive fringe coincidences between the displaced fringes in the image of the Nylon 6 fiber ($D = 1$) and undisplaced fringes of the same order of the empty interference field (liquid or fringes) equal to 1.0 over the whole spectrum ($q_s = 0.5,\ 0.0,\ -0.5$) as shown in Table 2. The correct value of the initial inteference order (m_1) can be checked using the well-known coefficient $B_{FC}\left(\frac{\delta_F}{\delta_C} \approx 1; \lambda_F = 486.1\,\text{nm} \text{ and } \lambda_C = 656.3\,\text{nm}\right)$ (degree of similarity of the spectral dispersions of the birefringence) [6]. Table 2 shows that the initial interference order ($m_1 = 2.0$) has been changed by -1.3 to obtain the correct dispersion curve as shown in Figure 3.

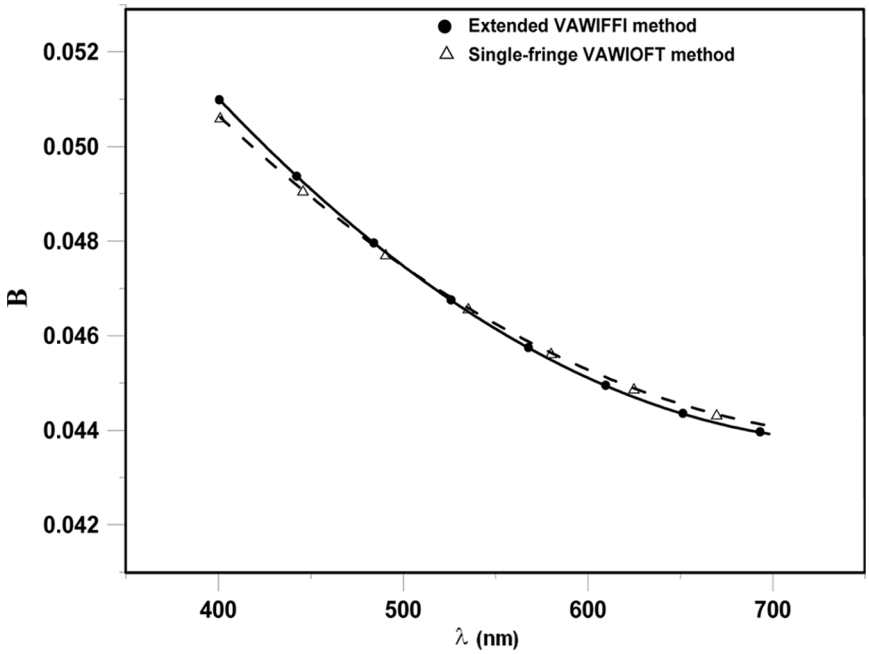

FIGURE 4 Spectral dispersion of the birefringence $B(\lambda)$ of the Nylon 6 fiber with a draw ratio 2.2 using extended VAWIFFI and single-VAWIOFT methods.

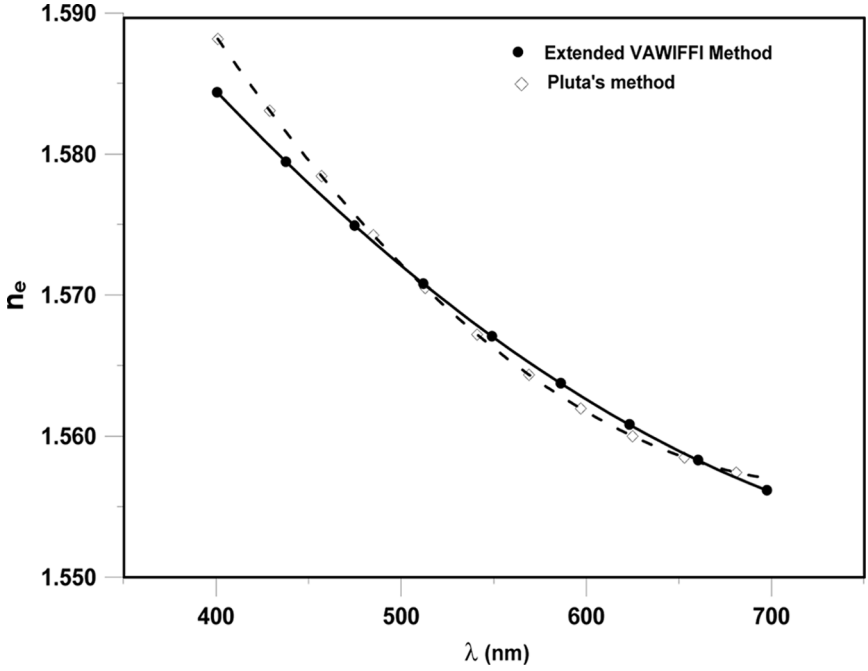

FIGURE 5 Spectral dispersion of the extraordinary refractive index $n_e(\lambda)$ of the Nylon 6 fiber with a draw ratio 2.2 using extended VAWIFFI and Pluta methods.

For this reason, the birefringence dispersion curves using the extended VAWIFFI and Pluta methods significantly diverged from each other. Moreover, the spectral dispersion of the refractive index $n_e(\lambda)$ of the Nylon 6 fiber with a draw ratio 2.2 using Pluta's method as shown in Figure 5. It is seen that the results obtained using the extended VAWIFFI and Pluta's method gives significantly different results.

TABLE 2 Results of the Measurement of the Initial Interference Order (m_1) and the Birefringence Dispersion of the Nylon 6 Fiber with a Draw Ratio 1.0 using Pluta's Method

q_s	λ (nm)	m_1	m_s	B
−0.5	645.94	3.117	1.5	0.0304
0.0	542.32	0.0	$m_1 = 2.0$	0.0340
0.5	475.02	3.529	2.5	0.0372

Average value of $m_1 = 3.32$.
Correct value of $m_1 = 2.0$.

Using Pluta's method, the global error in determining the birefringence δB (d, δ) and refractive index Δn (d, $n_{L,}$ δ) is estimated and found to be $\pm 10^{-3}$. Therefore, the coincident and anticoincident method (Pluta's method) does not require the determination of the initial interference order (m_1) when a weakly oriented polymeric object is investigated. In comparison with Pluta's method, the extended VAWIFFI method is more accurate, versatile and suitable for rapid determination of the weakly oriented polymeric object optical properties.

The optical system is adapted to conoscopic observation (VAWIOFT method) as shown in Figure 1. The weak birefringent Nylon 6 fiber is surrounded by air and oriented 45 degrees to the principal axes of the crossed polarizes. When the wavelength increases, the radius (r) of the visible dark fringe decreases toward the center of the microscope objective exit pupil. When the dark fringe appears in the center of the exit pupil, the next one emerges from the edge of the exit pupil. The radial difference (Δr) between two neighbor dark fringe radii depends on the wavelength, the focal length of the normal microscope objective and Nylon 6 birefringence, but the number of interference

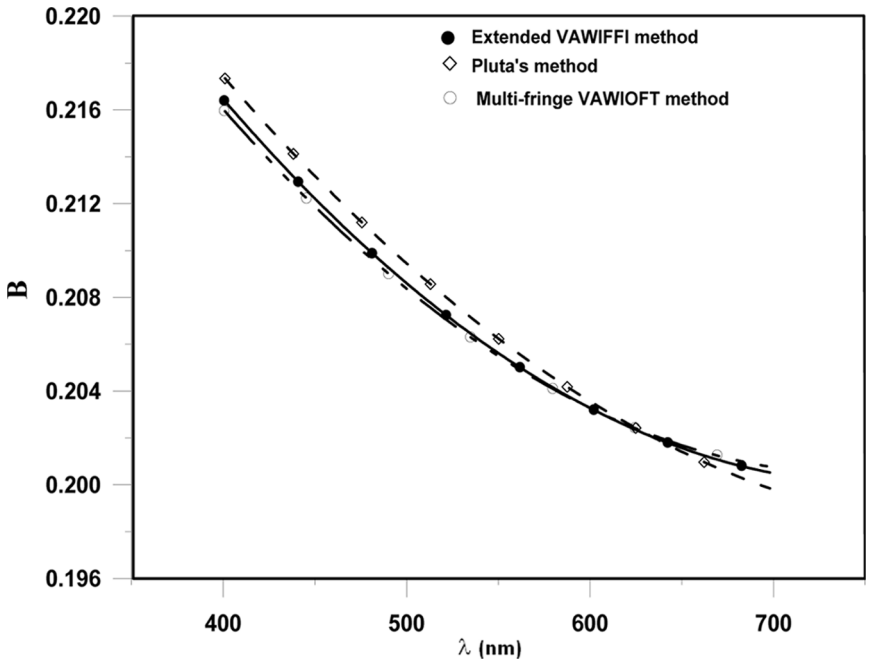

FIGURE 6 Spectral dispersion of the birefringence B(λ) of the aromatic polyamide fiber using extended VAWIFFI, multi-VAWIOFT and Pluta methods.

sequences depends only on the Nylon 6 birefringence. For Nylon 6 fibers, the number of the interference sequence is less than 2. This means that the radial difference is large and only one dark fringe is visible in the exit pupil over the whole visible spectrum when a normal microscope objective of magnifying and numerical apperature are less than, or equal to, 40x. In this case, the single-fringe VAWIOFT is applied [11]. The initial interference order (m_1) of Nylon 6 fibers with draw ratios 1.0 and 2.2 were determined and found to be 1.771 and 1.969, respectively. The spectral dispersions of the birefringence $B(\lambda)$ of these fibers can be determined using the single-fringe VAWIOFT method as shown in Figures 3 and 4. The accuracy of the birefringence measurement $\Delta B(d, \delta)$ is $\pm 21 \times 10^{-5}$. Using the extended VAWIFFI and single-fringe VAWIOFT methods, the initial interference order is more precisely calculated compared to the Pluta's method.

In order to confirm the illustration of the extended VAWIFFI method, the measurements have been performed on aromatic polyamide fiber of thickness 22.46 μm. The chain molecules of aromatic

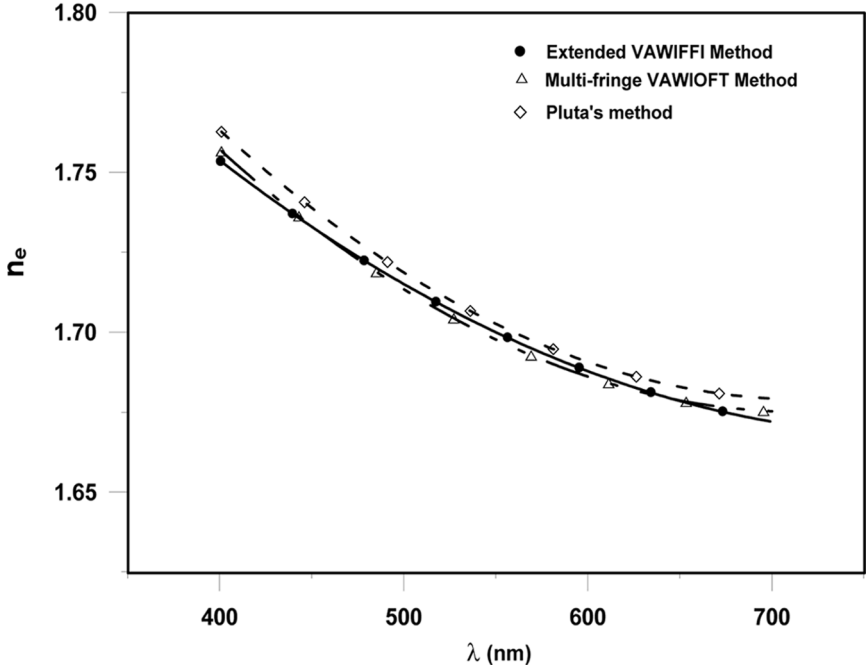

FIGURE 7 Spectral dispersion of extraordinary refractive index $n_e(\lambda)$ of the aromatic polyamide fiber using extended VAWIFFI, multi-VAWIOFT and Pluta methods.

polyamide fiber are highly oriented along the fiber axis; thus, the strength of the chemical bond can be exploited. The wavelength of monochromatic light can vary from the long to short region in the visible spectrum. Normal objective of a highly numerical aperture objective (objective magnification/numerical aperture: 60x/0.95) was used for observing two dark fringes in its exit pupil. The OFT and FFI patterns were automatically analyzed and processed. The radius of the annular dark fringes, fringe deflection (Z_s) and the interfringe spacing (h_s) of interference patterns corresponding to its wavelength were measured. Having measured $Z_s(\lambda)$ and $h_s(\lambda)$, the digital initial interference order was directly determined. Figures 6–8 demonstrate the comparison between the spectral dispersions of the aromatic polyamide fiber birefringence and directional refractive indices using the multi-fringe VAWIOFT [10], the extended VAWIFFI and Pluta's methods.

It is worth noting that there is not any uncertainty in identification of the interference orders using the current extended VAWIFFI method

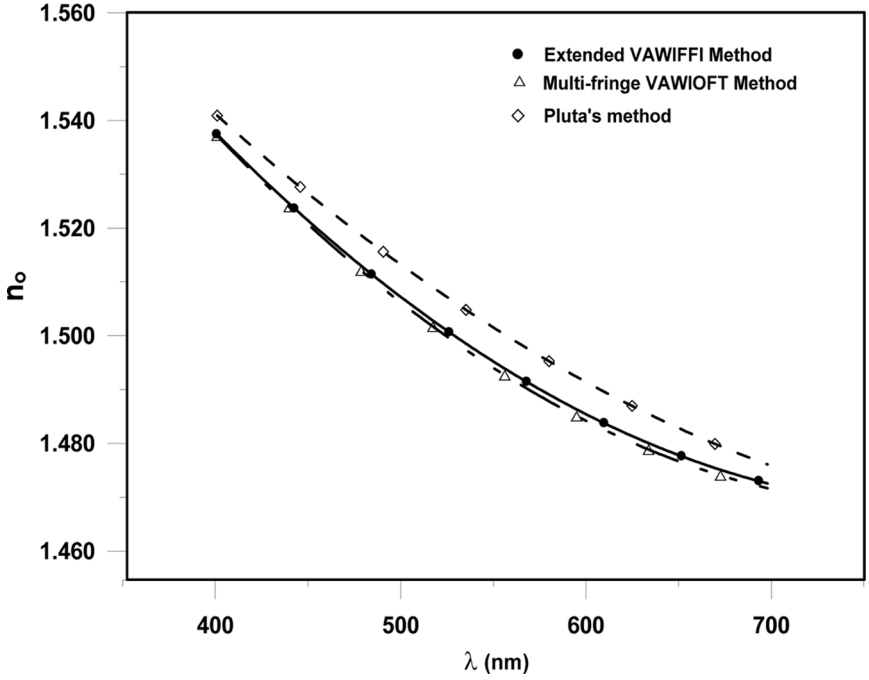

FIGURE 8 Spectral dispersion of ordinary refractive index $n_o(\lambda)$ of the aromatic polyamide fiber using extended VAWIFFI, multi-VAWIOFT and Pluta methods.

compared to the previous conventional VAWI methods [4,6,12]. It is not necessary to start or carry out the experiment at certain wavelengths. Also, there is no need to approximate the initial interference value. Furthermore, it overcomes the problem of chromaticity of the zero-order interference fringe displaced by the object under study.

CONCLUSION

- In the present work, an extended fringe field interference method is proposed for the determination of the initial and the current interference orders in weakly birefringent images over a small range of the visible spectrum.
- Using single- and multi-fringe VAWIOFT methods, there is no ambiguity in identification of the interference orders. So, these methods are used in this paper for a comparative study.
- The extended VAWIFFI method gives results very similar to single- and multi-fringe VAWIOFT methods.
- Using this extended VAWIFFI method there is no need to start with the initial coincident configuration as in traditional interferometric methods.
- Using this extended VAWIFFI method, the measuring accuracy of spectral dispersions of the birefringence and the refractive index of weak, moderate and highly birefringent objects is increased and is found to be $\pm 10^{-4}$.
- In the present paper, the variable-incident angle technique is used to increase the accuracy of measurement of the fiber thickness.
- The advantage of the extended VAWIFFI method is that it can be applied for all types of objects.

REFERENCES

[1] Bien, F., Camac, M., Caulfield, H. J., and Ezekiel, S. *Appl. Opt.* **20**, 400 (1981).
[2] Kerl, K. *Optica Acta* **26**, 1209 (1979).
[3] Gillard, C. W., Buholz, N., and Rider, D. W. *Opt. Eng.* **20**, 129 (1981).
[4] Pluta, M. (1993). *Advanced Light Microscopy*. Elsevier, Amsterdam, London, New York and Tokyo, p. 370.
[5] Matsuda, K., and Eiju, T. *Appl. Opt.* **25**, 2641 (1986).
[6] Pluta, M. *Journal of Microscopy* **149**, 97 (1988).
[7] Tiziani, H. J. *Optical Quantum Electron.* **21**, 253 (1989).
[8] Sadik, A. M., and Litwin D., *Inter. J. Polym. Mater.* **53**, 1015 (2004).
[9] Litwin, D., and Sadik, A. M. EOS Topical Meeting series, Diffraction Optics (DO'05), 62 (2005).
[10] Sadik, A. M. *Inter. J. Polym. Mater.* **58**, 243 (2009).

[11] Sadik, A. M., and Litwin, D. *Journal of Optics A: Pure Applied Optics* **4**, 135 (2002).
[12] Hamza, A. A., Belal, A. E., Sokkar, T. Z. N., El-Bakary, M. A., and Yassien, K. M. *Optics and Lasers in Engineering* **45**, 922 (2007).
[13] Sadik, A. M. *Measuring Science Technology* **18**, 2712 (2007).
[14] Trolinge, J. D., Chipman, R. A., and Wilson, D. K. *Opt. Eng.* **30**, 461 (1991).
[15] Mabrouk, M. A., and Sadik, A. M. *J. Polym. Mater.* **20**, 389 (2003).